International Journal of Applied Science and Engineering
2012. 10, 3: 181-207

Estimation of Structural Parameters Using Transfer Matrices and State Vectors

P. Nandakumar and K. Shankar*

Department of Mechanical Engineering, Indian Institute of Technology Madras, Chennai, India

Abstract: A new system identification (SI) method based on Transfer Matrix (TM) concept is proposed here to identify structural stiffness. Transfer matrices based on lumped mass and the more accurate consistent mass models are used here, based on displacement measurements in the time domain. The consistent mass based TM is derived from the dynamic stiffness matrix of a beam element. The state vector at a location is the sum of the internal and external contributions of displacements, forces and moments at that point - when multiplied with the (TM), we obtain the adjacent state vectors. The method of identification proposed here involves predicting the displacements at certain locations using the TM, and comparing them with the measured displacements at those locations. The mean square deviations between the measured and predicted responses at all locations are minimized using an optimization algorithm, and the optimization variables are the unknown stiffness parameters in the TM. A non-classical heuristic Particle Swarm Optimization algorithm (PSO) is used, since it is especially suited for global search. Different strategies for calculating the initial state vector, as well as two identification processes *viz.,* simultaneous and successive methods, are discussed. Numerical simulations are carried out on four examples ranging from a simple spring mass system to a nine member framed structure. The speed and accuracy of identification using this method are good. One main advantage of this method is that it can be applied at any portion of the structure to identify the local parameters in that zone without the need to model the entire global structure.

Keywords: Structural identification; transfer matrix; simultaneous identification; successive identification; particle swarm optimization.

1. Introduction

System Identification (SI) is usually an inverse process by which structural parameters are identified from input excitation and its output responses. SI plays an important role in updating the model so as to better predict structural response. For structural control applications, identification of actual parameters is also essential for effective control.

It can be used for structural health monitoring and damage assessment in a non-destructive way by tracking changes in structural parameters such as buildings and bridges, in assessment of these structures after natural disasters, and in evaluation of effectiveness of retrofitting/repair measures. From computational point of view, structural identification presents a challenging prob-

* Corresponding author; e-mail: skris@iitm.ac.in

Received 19 December 2011
Revised 6 February 2012
Accepted 8 February 2012

lem particularly when the system involves a large number of unknown parameters. Besides accuracy and efficiency, robustness is an important issue for selecting the identification strategy. Research interest in this subject area has increased steadily over the years, mainly due to rapid enhancement in computer power and development in new algorithms. A review of up-to-date literature is presented here as per the following frame work. a) existing SI methods. b) time domain methods (classical and non-classical approaches) c) application of Particle swarm and Genetic Algorithm, d) substructure and global approaches, e) Transfer Matrix method and its relation to substructure method. All these areas are relevant to the proposed topic of this paper, which is a non-classical time domain method with some features of substructure identification.

SI algorithms are classified as static or dynamic (*i.e.,* vibration based) [1,2]. Due to the non-uniqueness of identification and the difficulty in measuring static displacements under small loads, vibration based methods are usually preferred. Hence either frequency domain or time domain SI is widely used. Frequency domain SI algorithms have been developed more widely in last three decades, since the data are conveniently transformed from time domain to natural frequencies, mode shapes and frequency response functions. Maia and Silva [3] have presented some modal analysis techniques for identification. Ma and Eric [4] identified damage on structures like cantilever, ten story steel frame and plates by comparing natural frequencies of the undamaged and damaged structures. Jinhee [5] identified cracks in a cantilever using vibration amplitudes in the frequency domain. But comparison of limited sets of modal parameters reduces the accuracy of identification of complex structures in the frequency domain.

A few time domain methods are reviewed here. They use the measured accelerations or velocities or displacements of the structure directly without transformation to the frequency domain. Time domain algorithms are also categorized as based on Classical or Non-classical methods of convergence, for minimizing the errors between the measured responses and predicted responses from an analytical model which is iteratively updated. A few classical methods are presented here as follows. Ghanem and Shinozuka [6] have reported a few classical SI techniques such as Recursive Least Square method (RLS), Extended Kalman Filter method (EKF), maximum likelihood method, recursive instrumental variable. Petsounis and Fassois [7] have compared some stochastic algorithms like Prediction Error Method (PEM), two stage LS method, Instrumental Variable method with a few deterministic algorithms like Prony method, Eigen system Realization Algorithm (ERA), LS methods based on identification results of a linear two-dimensional model of one-half of a railway structure. Studies such as Caravani *et al*. [8], Masaru and Etsuro [9], Shinozuka *et al.* [10] used some of the above classical methods. Lus *et al*. [11] and Angelis *et al.* [12] identified modal damping and structural parameters using a two stage approach of OKID (Observer Kalman-Filter Identification) and ERA method. In general, the classical methods such as above work appear to well when the number of unknowns is few and measurement noise level is negligible. They are also computationally intensive.

The non-classical methods in time domain identification are briefly discussed next. The shortcomings of the classical methods are a) they require the calculation of first and higher derivatives of its objective function, and b) there is a possibility of converging to the local optima and c) some classical methods require a good initial guess of the unknown parameters to start the iterations. When the system involves a large number of

unknown parameters, non-classical algorithms such as Genetic Algorithm (GA) and Particle Swarm Optimization (PSO) algorithm produce better results in minimizing the deviation between measured and predicted values. A non-classical method is usually based on heuristic concepts such as Evolutionary principle (GA) or Behavioral principle (PSO), without the requirement to calculate any derivatives. PSO was developed more than a decade later than GA and proved to be simpler, more accurate and faster. Kennedy and Eberhart [13] developed the PSO algorithm for optimization of problems with many variables. Mouser and Dunn [14] have compared performance of PSO and GA, proved that PSO is much superior to GA and easy to configure. Qie *et al* [15] used PSO and GA for parameter estimation and proved that PSO is better than GA. Perez and Behdinan [16] also used PSO for a structural identification problem of 72 bar truss with good accuracy. Koh *et al* [17] identified a maximum of 52 structural parameters using GA with a hybrid local search method. GA directs the search toward the global optima and the local search improves the convergence. Begambre and Laier [18] detected damage in a truss and a free-free beam using Particle Swarm Optimization (PSO) with a simplex hybrid strategy. Hesheng *et al* [19] applied Differential Evolution (DE) to a 20 DOF system and observed improvements when compared with GA and PSO.

A recent improvement in time domain identification is the substructure approach, as opposed to identifying the complete global model. Koh *et al.* [20,21] explained a divide-and-conquer strategy based on sub-structure approach. The whole structure is divided into many small sub-structures, and identification is done on only one substructure at a time; thus the number of unknowns involved is fewer and hence the numerical accuracy is better than the global approach. Sandesh and Shankar [22] identified crack damage in a thin plate with the sub-structure approach using GA and PSO hybrids. Tee *et al.* [23] identified damage in a 50 DOF structure with sub-structure approach using Condensed Model Identification and Recovery (CMIR) method based on OKID/ERA method and GA where fixed sensor and repositioned sensor approaches are adopted.

A novel Transfer Matrix method of system identification is proposed here as an alternative to the time domain method using substructures *i.e.,* it is a local method of identification where only the local properties need to be known. Transfer matrices and state vectors are introduced here for system identification which are independent of the number of DOF of the global structure. Hence there is a significant saving in computational effort using this method. Transfer matrix method of SI can be applied at a point anywhere in the structure once the initial state vector at a nearby point is known.

A brief review of Transfer matrices, their origins and application is presented here. Steidel [24] derived the transfer matrix for a spring mass system with one DOF and a beam element. The transfer matrix for the beam element is derived by assuming that the mass is concentrated only at end nodes and the beam element is mass less throughout its length. Using the transfer matrix natural frequencies of a two DOF spring mass system and a cantilever with end mass are determined. Meirovitch [25] determined the natural frequencies and mode shapes of a non-uniform pinned-pinned beam with ten elements using transfer matrix by assuming the lumped mass at the end nodes of the beam element. Nandakumar and Shankar [26] used a transfer matrix and state vectors for the first time for an inverse problem in the time domain and identified stiffness of a cantilever by assuming mass is concentrated

at the end nodes, however this approximation results in the agreement of only the first few natural frequencies. Khiem and Lien [27] carried out natural frequency analysis on a beam with arbitrary number of cracks using transfer matrix method. Tuma and Cheng [28] derived an improved transfer matrix for beam element with an assumption of the mass of the beam element is concentrated at its mass center and the element is mass less at both sides of the mass center. It is found that there is a good improvement in natural frequencies when the above suggestion is adopted. But still there is a considerable error in natural frequencies at higher modes. Walter and Walter [29] explained the derivation of transfer matrix from stiffness matrix for static applications. Based on this, a new transfer matrix is derived from dynamic stiffness matrix (using consistent mass matrix) of the beam element which results the natural frequencies of the structure are very close to its exact value.

In this paper, both lumped mass transfer matrix and consistent mass transfer matrix are used for structural system identification. Based on the author's literature survey of existing SI methods, no studies using transfer matrix and state vectors for inverse problems have been found. Hence in this paper a new method based on the Transfer matrix and State vectors is proposed to identify stiffnesses of the structure.

2. Transfer matrices and state vectors

A state vector at a point in the structure contains the output responses such as displacement, and rotation (angular displacement) and the net forces and moments, which is the summation of internal and external contributions. The Transfer matrix (TM) is a square matrix which contains the structural parameters such as mass, stiffness and also the circular frequency of vibration. When the state vector at one location is multiplied by the TM of an element of length *l*, we obtain the state vector at the new location distance *l* from the starting vector.

2.1. Spring-mass system

The TM of simple spring mass system is discussed in [24] and is briefly presented here (see Figure 1). The spring mass system is divided into the spring (*a*-*b*) and mass (*b*-*c*). The plane '*c*' is considered at the free end of the mass, the plane '*a*' is considered at the fixed end of the spring and the plane '*b*' is considered at the connecting point of mass and spring. The system is excited by a harmonic force *F(t)*with a circular frequency of ω at the plane *c*. The mass vibrates with a displacement $x_c(t)$. If *k* and *m* are the stiffness and mass of the spring, the state vector at plane *c* is given by $\{X_c\} = \{X_{ci}\} + \{X_{ce}\}$ where $\{X_{ci}\} = \{x_c(t);\ f_c(t)\}^T$ the internal component vector and $\{X_{ce}\} = \{0;\ F(t)\ \}^T$ is external component vector. The transfer matrix which transfers the state vector from the plane '*c*' to plane *'b'* is known as *Point transfer matrix* [*M*] and obtained by applying the Newton's second law on the mass element.

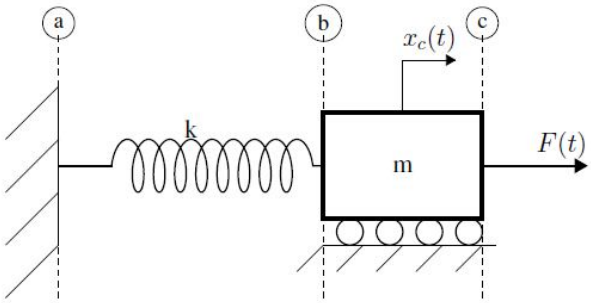

Figure 1. Spring mass system

Displacement at plane $b\ x_b(t) = x_c(t)$ (1)

Force at the plane *b*

$$f_b(t) = -m\ddot{x}_c(t) + f_c(t) + F(t) \quad (2)$$

Where $\ddot{x}_c(t)$ is acceleration of the mass at the plane c, also $\ddot{x}_c(t) = -\omega^2 x_c(t)$; Writing the above Eq.1 and 2 in matrix

form,

$$\begin{Bmatrix} x_b(t) \\ f_b(t) \end{Bmatrix} = \begin{bmatrix} 1 & 0 \\ m\omega^2 & 1 \end{bmatrix} \left(\begin{Bmatrix} x_c(t) \\ f_c(t) \end{Bmatrix} + \begin{Bmatrix} 0 \\ F(t) \end{Bmatrix} \right) \quad (3)$$

Eq.3 can be written as $\{X_{bi}\}=[M]\{X_c\}$, where $\{X_{bi}\}$ is internal response vector at the plane *b*. and the point transfer matrix $[M]$ is given by,

$$[M] = \begin{bmatrix} 1 & 0 \\ m\omega^2 & 1 \end{bmatrix} \quad (4)$$

The transfer matrix which transfers the state vector from the plane '*b*' to plane *'a'* is known as *field transfer matrix* $[K]$ and obtained by writing the static equilibrium equation for the spring element.

$$f_a(t) = f_b(t) = k(x_b(t) - x_a(t)) \quad (5)$$

$$x_a(t) = x_b(t) - \frac{f_b(t)}{k} \quad (6)$$

Writing Eq.5 and Eq.6 in matrix form

$$\begin{Bmatrix} x_a(t) \\ f_a(t) \end{Bmatrix} = \begin{bmatrix} 1 & \frac{-1}{k} \\ 0 & 1 \end{bmatrix} \begin{Bmatrix} x_b(t) \\ f_b(t) \end{Bmatrix} \quad (7)$$

Eq.7 can be written as $\{X_{ai}\} = [K]\{X_{bi}\}$,where $[K]$ is field transfer matrix which is given by

$$[K] = \begin{bmatrix} 1 & \frac{-1}{k} \\ 0 & 1 \end{bmatrix} \quad (8)$$

The overall transfer matrix which transfers state vector from the plane *c* to *a* can be obtained by substituting Eq.3 in Eq.7

$$\{X_{ai}\}=[K][M]\{X_c\} \quad (9)$$

$\{X_{ai}\}=[T]\{X_c\}$ where $[T]=[K][M]$ is overall transfer matrix for the system.

$$[T] = \begin{bmatrix} 1 - \frac{m\omega^2}{k} & \frac{-1}{k} \\ m\omega^2 & 1 \end{bmatrix} \quad (10)$$

2.2. Transfer matrix for beam elements

As explained in section.1 the transverse vibration of beams can be studied using transfer matrices. Steidel [24] and Meirovitch [25] derived transfer matrices for a beam element by assuming that the mass is concentrated at the two end nodes (two point mass representation) and the beam element is assumed to be mass-less throughout its length. There is appreciable error in predicting the natural frequencies of continuous systems using this method. Tuma and Cheng [28] derived an improved transfer matrix for a beam element with the assumption that the mass of the beam element is concentrated at its mass center (single point mass representation) and the element is mass-less on either sides of the mass center as shown in Figure 2 (a). It is found there is an improvement in the prediction of natural frequencies using this approach but there is a significant error in the higher frequencies. A new transfer matrix formulation is derived here from the dynamic stiffness matrix of a beam element based on its consistent mass matrix (Consistent Mass Transfer Matrix - CMTM) which gives more improved results. The single point transfer matrix and consistent mass transfer matrix are used in this paper for structural stiffness identification, and their derivation is very briefly discussed here.

2.2.1. TM with single point mass

The beam element with mass lumped at its mass center (Single point mass) is shown in Figure 2 (a) and the TM has been calculated in [28]. Let $y_1(t)$be the vertical displacement, $\theta_1(t)$be the angular displacement, $M_1(t)$ be the bending moment, $\mu_1(t)$ be the external moment,$V_1(t)$be the shear force and $F_1(t)$be the external force at the node *1*. The state vector for the node*1* is $\{X_1\} = \{X_{1i}\}+\{X_{1e}\}$ where $\{X_{1i}\} = \{y_1(t), \theta_1(t), M_1(t), V_1(t)\}^T$ is internal response vector and $\{X_{1e}\} = \{0; 0; \mu_1(t); F_1(t)\}^T$is external force vector. The field transfer matrix $[K]$ for a beam element shown in Figure 2 (b) of length l_e without con-sidering mass is determined first; then the effect of the lumped mass element is

considered. The responses at the node *2* of the beam element can be written in terms of the same at the node *1* as shown below.

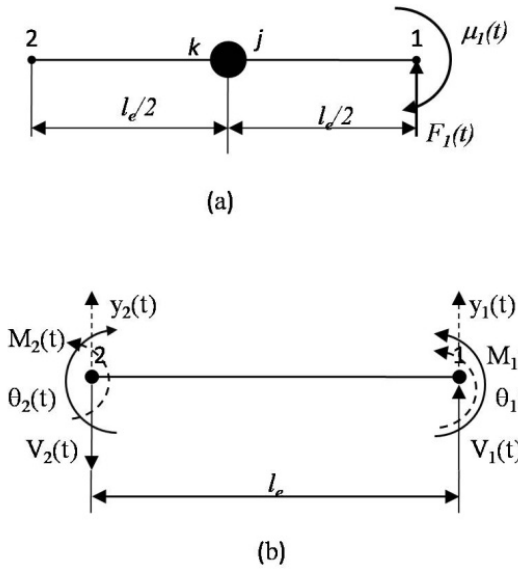

Figure 2. Beam element (a) Single point mass (b) Consistent mass

$$y_2(t) = y_1(t) - l_e\theta_1(t) + \frac{l_e^2}{2EI}M_1(t) + \frac{l_e^3}{6EI}V_1(t)$$

$$\theta_2(t) = \theta_1(t) - \frac{l_e}{EI}M_1(t) - \frac{l_e^2}{2EI}V_1(t)$$

$$M_2(t) = M_1(t) + \mu_1(t) + l_eV_1(t) + l_eF_1(t)$$

$$V_2(t) = V_1(t) + F_1(t) \tag{11}$$

Where l_e is the length of the element, E is Young's modulus of the beam material and I is area moment of inertia of the beam section. The system of Eq.11 can be written in matrix form,

$$\begin{Bmatrix} y_2(t) \\ \theta_2(t) \\ M_2(t) \\ V_2(t) \end{Bmatrix} = \begin{bmatrix} 1 & -l_e & \frac{l_e^2}{2EI} & \frac{l_e^3}{6EI} \\ 0 & 1 & -\frac{l_e}{EI} & \frac{-l_e^2}{2EI} \\ 0 & 0 & 1 & le \\ 0 & 0 & 0 & 1 \end{bmatrix} \left\{ \begin{Bmatrix} y_1(t) \\ \theta_1(t) \\ M_1(t) \\ V_1(t) \end{Bmatrix} + \begin{Bmatrix} 0 \\ 0 \\ \mu_1(t) \\ F_1(t) \end{Bmatrix} \right\} \tag{12}$$

Eq.12 can be written as $\{X_{2i}\} = [K]\{X_1\}$, where the field transfer matrix $[K]$ is given by

$$[K]=\begin{bmatrix} 1 & -l_e & \frac{l_e^2}{2EI} & \frac{l_e^3}{6EI} \\ 0 & 1 & -\frac{l_e}{EI} & \frac{-l_e^2}{2EI} \\ 0 & 0 & 1 & le \\ 0 & 0 & 0 & 1 \end{bmatrix} \tag{13}$$

The point transfer matrix [*M*] of the point mass can be obtained as explained in section 2.1,

$$[M]=\begin{bmatrix} 1 & 0 & 0 & 0 \\ 0 & 1 & 0 & 0 \\ 0 & 0 & 1 & 0 \\ m\omega^2 & 0 & 0 & 1 \end{bmatrix} \tag{14}$$

The beam element (single point mass) shown in Figure 2 (a) is divided into three elements such as two mass less spring elements (*2-k*) and (*j-1*) and one mass element (*k-j*). The field transfer matrix [*K'*] for the half length of the element is given by substituting the element length as $l_e/2$.

$$[K']=\begin{bmatrix} 1 & \frac{-l_e}{2} & \frac{l_e^2}{8EI} & \frac{l_e^3}{48EI} \\ 0 & 1 & -\frac{l_e}{2EI} & \frac{-l_e^2}{8EI} \\ 0 & 0 & 1 & \frac{le}{2} \\ 0 & 0 & 0 & 1 \end{bmatrix} \tag{15}$$

It is assumed that state vector at node *1* is known and then the following relations can be obtained.

$\{X_{ji}\}=[K']\{X_1\}$; $\{X_{ki}\}=[M]\{X_{ji}\}$ and $\{X_{2i}\}=[K']\{X_{ki}\}$, hence, the state vector at the node *2* in terms of node *1* can be directly obtained by $\{X_{2i}\}=[K'][M][K']\{X_1\}$, from this, the overall transfer matrix for the beam element is obtained as $[T]=[K'][M][K']$.

$$[T]=\begin{bmatrix} 1+\frac{m\omega^2 l_e^3}{48EI} & -l_e-\frac{m\omega^2 l_e^4}{96EI} & \frac{m\omega^2 l_e^5}{384(EI)^2}+\frac{l_e^2}{2EI} & \frac{m\omega^2 l_e^6}{2304(EI)^2}+\frac{l_e^3}{6EI} \\ -\frac{m\omega^2 l_e^2}{8EI} & 1+\frac{m\omega^2 l_e^3}{16EI} & -\frac{m\omega^2 l_e^4}{64(EI)^2}-\frac{l_e}{EI} & -\frac{m\omega^2 l_e^5}{384(EI)^2}-\frac{l_e^2}{2EI} \\ \frac{m\omega^2 l_e}{2} & -\frac{m\omega^2 l_e^2}{4} & 1+\frac{m\omega^2 l_e^3}{16EI} & l_e+\frac{m\omega^2 l_e^4}{96EI} \\ m\omega^2 & -\frac{m\omega^2 l_e}{2} & \frac{m\omega^2 l_e^2}{8EI} & 1+\frac{m\omega^2 l_e^3}{48EI} \end{bmatrix} \tag{16}$$

Usually the subscript *i* is omitted from the state vector representations and the form $\{X_2\}=[T]\ \{X_1\}$ is frequently used in literature.

2.2.2. Consistent mass transfer matrix (CMTM)

The CMTM is newly derived in this paper and used for accurate identification of beams and frames. The characteristic equation of a linear dynamic system is given by

$$[M]\{\ddot{x}(t)\}+[C]\{\dot{x}(t)\}+[K]\{x(t)\}=\{f(t)\} \tag{17}$$

Where [*M*] is consistent mass matrix, [*C*] is damping matrix, [*K*] is stiffness matrix, $\ddot{x}(t)$, $\dot{x}(t)$, *x(t)*and *f(t)* are acceleration, velocity, displacement and external force vectors respectively. For lightly damped structures/materials, the damping force is negligible when compared with other forces. Hence,

$$[M]\{\ddot{x}(t)\}+[K]\{x(t)\}=\{f(t)\} \tag{18}$$

also $\ddot{x}(t)=-\omega^2 x(t)$ where ω is frequency of excitation in *r/s*. Substitute in Eq.18,

$$([K]-\omega^2[M])\{x(t)\}=\{f(t)\} \tag{19}$$

Let [*D*] = [*K*] - ω^2[*M*] called dynamic stiffness matrix. The Eq.19 becomes,

$$[D]\{x(t)\}=\{f(t)\} \tag{20}$$

Consider an one dimensional Euler-Bernoulli beam element with two end nodes as shown in Figure 2 (b), the elemental stiffness matrix is

$$[K]=\frac{EI}{l_e^3}\begin{bmatrix} 12 & 6l_e & -12 & 6l_e \\ & 4l_e^2 & -6l_e & 2l_e^2 \\ & & 12 & -6l_e \\ & sym & & 4l_e^2 \end{bmatrix}$$

and elemental consistent mass matrix is

$$[M]=\frac{\rho A l_e}{420}\begin{bmatrix} 156 & 22l_e & 54 & -13l_e \\ & 4l_e^2 & 13l_e & -3l_e^2 \\ & & 156 & -22l_e \\ & sym & & 4l_e^2 \end{bmatrix}$$

Since the beam element is in dynamic equilibrium, the Eq.20. is written as,

$$\begin{Bmatrix} -V_1(t) \\ -M_1(t) \\ \hline V_2(t) \\ M_2(t) \end{Bmatrix}=\left[\begin{array}{cc|cc} D_{11} & D_{12} & D_{13} & D_{14} \\ D_{21} & D_{22} & D_{23} & D_{24} \\ \hline D_{31} & D_{32} & D_{33} & D_{34} \\ D_{41} & D_{42} & D_{43} & D_{44} \end{array}\right]\begin{Bmatrix} y_1(t) \\ \theta_1(t) \\ \hline y_2(t) \\ \theta_2(t) \end{Bmatrix} \tag{21}$$

Where [D]=[*K*] - ω^2[*M*]. The state vector at node 1 $\{X_{1i}\} = \{y_1(t);\ \theta_1(t);\ M_1(t);\ V_1(t)\}^T$ is known which can be obtained by rearranging the force and displacement vectors of Eq.21. Since the external forces are zero, $\{X_1\}=\{X_{1i}\}$.

$$\text{Let}[A]=\begin{bmatrix} D_{21} & D_{22} \\ D_{11} & D_{12} \end{bmatrix},\ [B]=\begin{bmatrix} D_{23} & D_{24} \\ D_{13} & D_{14} \end{bmatrix},\ [C]=\begin{bmatrix} D_{41} & D_{42} \\ D_{31} & D_{32} \end{bmatrix},\ [E]=\begin{bmatrix} D_{43} & D_{44} \\ D_{33} & D_{34} \end{bmatrix},$$

$$\{F(t)\}=\begin{Bmatrix} M(t) \\ V(t) \end{Bmatrix}\text{and}\{x(t)\}=\begin{Bmatrix} y(t) \\ \theta(t) \end{Bmatrix}\ \text{ then the Eq.21 is written as,}$$

$$\begin{Bmatrix} -F_1(t) \\ F_2(t) \end{Bmatrix}=\begin{bmatrix} [A] & [B] \\ [C\} & [E] \end{bmatrix}\begin{Bmatrix} x_1(t) \\ x_2(t) \end{Bmatrix} \tag{22}$$

Rearranging the Eq.22,

$$\begin{bmatrix} -[B] & [0] \\ -[E] & [I] \end{bmatrix}\begin{Bmatrix} x_2(t) \\ F_2(t) \end{Bmatrix}=\begin{bmatrix} [A] & [I] \\ [C] & [0] \end{bmatrix}\begin{Bmatrix} x_1(t) \\ F_1(t) \end{Bmatrix} \tag{23}$$

Where [I] is an identity matrix of size 2 × 2 and [0] is null matrix of size 2 × 2.

$$\begin{Bmatrix} x_2(t) \\ F_2(t) \end{Bmatrix} = \begin{bmatrix} -[B] & [0] \\ -[E] & [I] \end{bmatrix}^{-1} \begin{bmatrix} [A] & [I] \\ [C] & [0] \end{bmatrix} \begin{Bmatrix} x_1(t) \\ F_1(t) \end{Bmatrix} \tag{24}$$

From the Eq.24 the consistent mass transfer matrix (CMTM) is obtained

$$[T] = \begin{bmatrix} -[B] & [0] \\ -[E] & [I] \end{bmatrix}^{-1} \begin{bmatrix} [A] & [I] \\ [C] & [0] \end{bmatrix} \tag{25}$$

The elements of the CMTM are given below.

$$T_{11} = 26 - \frac{5400EI(m\omega^2 l_e^3 + 1400EI)}{302400(EI)^2 + 720m\omega^2 l_e^3 EI + (m\omega^2 l_e^3)^2}$$

$$T_{12} = \frac{1800EIl_e(168EI - m\omega^2 l_e^3)}{302400(EI)^2 + 720m\omega^2 l_e^3 EI + (m\omega^2 l_e^3)^2} - 2l_e$$

$$T_{13} = \frac{60l_e^2(13m\omega^2 l_e^3 + 2520EI)}{302400(EI)^2 + 720m\omega^2 l_e^3 EI + (m\omega^2 l_e^3)^2}$$

$$T_{14} = \frac{180l_e^3(13m\omega^2 l_e^3 + 280EI)}{302400(EI)^2 + 720m\omega^2 l_e^3 EI + (m\omega^2 l_e^3)^2}$$

$$T_{21} = \frac{-120m\omega^2 l_e^2(m\omega^2 l_e^3 + 420EI)}{302400(EI)^2 + 720m\omega^2 l_e^3 EI + (m\omega^2 l_e^3)^2}$$

$$T_{22} = 10 - \frac{360EI(7560EI - 17m\omega^2 l_e^3)}{302400(EI)^2 + 720m\omega^2 l_e^3 EI + (m\omega^2 l_e^3)^2}$$

$$T_{23} = \frac{-1080l_e(3m\omega^2 l_e^3 + 280EI)}{302400(EI)^2 + 720m\omega^2 l_e^3 EI + (m\omega^2 l_e^3)^2}$$

$$T_{24} = \frac{-60l_e^2(13m\omega^2 l_e^3 + 2520EI)}{302400(EI)^2 + 720m\omega^2 l_e^3 EI + (m\omega^2 l_e^3)^2}$$

$$T_{31} = \frac{m\omega^2 l_e(604800(EI)^2 + 2280m\omega^2 l_e^3 EI + (m\omega^2 l_e^3)^2)}{4(302400(EI)^2 + 720m\omega^2 l_e^3 EI + (m\omega^2 l_e^3)^2)}$$

$$T_{32} = \frac{-m\omega^2 l_e^2(3024000(EI)^2 + 4680m\omega^2 l_e^3 EI + (m\omega^2 l_e^3)^2)}{60(302400(EI)^2 + 720m\omega^2 l_e^3 EI + (m\omega^2 l_e^3)^2)}$$

$$T_{33} = 10 - \frac{360EI(7560EI - 17m\omega^2 l_e^3)}{302400(EI)^2 + 720m\omega^2 l_e^3 EI + (m\omega^2 l_e^3)^2}$$

$$T_{34} = 2l_e - \frac{1800EIl_e(168EI - m\omega^2 l_e^3)}{302400(EI)^2 + 720m\omega^2 l_e^3 EI + (m\omega^2 l_e^3)^2}$$

$$T_{41} = \frac{m\omega^2(604800(EI)^2 + 5640m\omega^2 l_e^3 EI + 7(m\omega^2 l_e^3)^2)}{2(302400(EI)^2 + 720m\omega^2 l_e^3 EI + (m\omega^2 l_e^3)^2)}$$

$$T_{42} = -\frac{m\omega^2 l_e(604800(EI)^2 + 2280m\omega^2 l_e^3 EI + (m\omega^2 l_e^3)^2)}{4(302400(EI)^2 + 720m\omega^2 l_e^3 EI + (m\omega^2 l_e^3)^2)}$$

$$T_{43} = \frac{120m\omega^2 l_e^2(m\omega^2 l_e^3 + 420EI)}{302400(EI)^2 + 720m\omega^2 l_e^3 EI + (m\omega^2 l_e^3)^2}$$

$$T_{44} = 26 - \frac{5400EI(m\omega^2 l_e^3 + 1400EI)}{302400(EI)^2 + 720m\omega^2 l_e^3 EI + (m\omega^2 l_e^3)^2}$$

2.3. Transfer matrix and state vector for the global structure

Calculation of state vector at any node of a global structure, from one known initial state vector at a given node using transfer matrices is illustrated here. For example, a cantilever is considered with '*n*' nodes subjected to arbitrary point loading as shown in Figure 3.

It is assumed that the state vector at the node *1*is known (the initial state vector $\{X_1\}$). The state vectors at other nodes can be calculated by successive multiplication of elemental transfer matrices. Let $\{X_{1i}\}$ and $\{X_{1e}\}$ be the internal response vector and external force vector respectively at node *1*, $[T_{1,2}]$ is transfer matrix which transfers the state vector $\{X_1\}=\{X_{1i}\}+\{X_{1e}\}$into internal response vector $\{X_{2i}\}$ at node *2*. For the first element formed by nodes *1* and *2*, the relation between state vectors and transfer matrix can be written as follows.

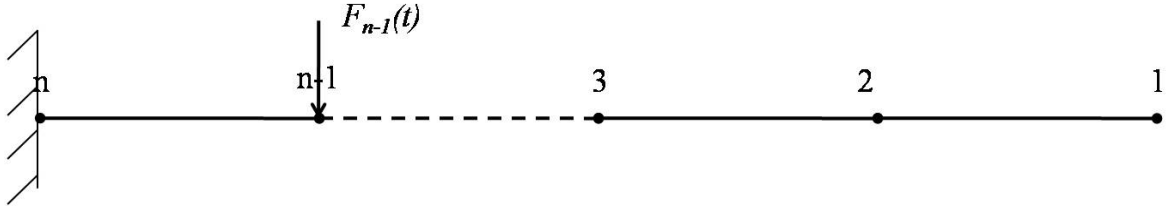

Figure 3. Cantilever with arbitrary point loading

$$\{X_{2i}\} = [T_{1,2}](\{X_{1i}\} + \{X_{1e}\}) \tag{26}$$

In general, for (n-1)th element, the state vector at the node n can be obtained as follows.

$$\{X_{ni}\} = [T_{n-1,n}](\{X_{(n-1)i}\} + \{X_{(n-1)e}\}) \tag{27}$$

From the above equations, the internal response vector $\{X_{ni}\}$ at the node '*n*' can be calculated

from initial state vector $\{X_{1i}\}$ and external force vectors at all nodes as follows.

$$\{X_{ni}\} = \left(\prod_{k=1}^{n-1} [T_{(n-k),(n+1-k)}] \right) \{X_{1i}\} + \sum_{j=1}^{n-1} \left(\prod_{k=1}^{n-j} [T_{(n-k),(n+1-k)}] \right) \{X_{je}\} \quad (28)$$

For free vibration of cantilever *i.e* without any external forces, as a special case the Eq.28 can be deduced as

$$\{X_n\} = \left(\prod_{k=1}^{n-1} [T_{(n-k),(n+1-k)}] \right) \{X_1\} \quad (29)$$

In the above equation, $[T_{1,n}^G] = \prod_{k=1}^{n-1} [T_{(n-k),(n+1-k)}]$ is known as global transfer matrix of the structure which is obtained by progressive pre-multiplication of elemental transfer matrices.

3. Comparison of various TM's for beam elements

The accuracy of TM's based on two point lumped mass method, single point lumped mass method and consistent mass are compared by checking the accuracy of the natural frequencies predicted by them, and verifying these with the analytically predicted natural frequency based on distributed mass (continuous system) model. A steel cantilever of size *24.6* × *5.7* × *350* mm, flexural rigidity (*EI*) 75.93 N.m^2 and fixed at its one end as shown in Figure 3. For free vibration of cantilever the external force vector is zero, the global transfer matrix and the relation between free end to fixed end state vectors can be obtained from the Eq.29. Since no external force is applied, the shear force and bending moment at the free end is zero. The displacement and rotation responses at the fixed end are zero. The forcing and boundary conditions are applied on the state vectors. Then Eq.29 becomes

Table 1. Natural frequencies of cantilever in Hz

Exact Values	Two point Lumped mass TM	Single point Lumped mass TM	Consistent mass TM
38.33	33.53	38.51	38.33
240.21	212.24	244.17	240.24
672.60	599.14	690.39	673.29
1318.02	1179.12	1361.97	1322.89

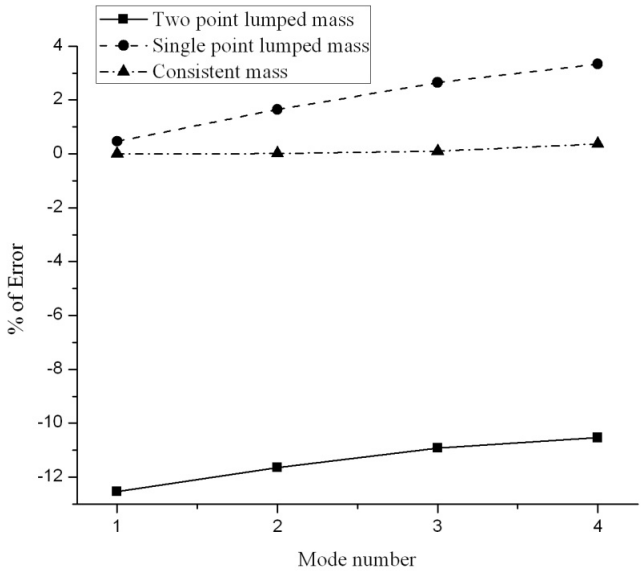

Figure 4. Variation of percentage of error in natural frequencies

$$\begin{Bmatrix} 0 \\ 0 \\ M_n(t) \\ V_n(t) \end{Bmatrix} = [T^G_{1,n}] \begin{Bmatrix} y_1(t) \\ \theta_1(t) \\ 0 \\ 0 \end{Bmatrix} \tag{30}$$

The Eq.30 consists of four equations, out of which first two equations can be written as shown in Eq.31.

$$\begin{bmatrix} T^G_{11} & T^G_{12} \\ T^G_{21} & T^G_{22} \end{bmatrix} \begin{Bmatrix} y_1(t) \\ \theta_1(t) \end{Bmatrix} = \begin{Bmatrix} 0 \\ 0 \end{Bmatrix} \tag{31}$$

$$\begin{vmatrix} T^G_{11} & T^G_{12} \\ T^G_{21} & T^G_{22} \end{vmatrix} = 0 \tag{32}$$

The Eq.32 is solved and gives natural frequencies of the system. The calculated natural frequencies for the first four modes by different methods are tabulated in Hz in Table 1 and the error variation for different types of TM is shown in Figure 4. From the graph, it is clearly seen that the natural frequencies determined by consistent mass transfer matrix (CMTM) have errors close to zero. The error is largest for the two point mass TM and moderate for the single point mass TM. Hence it is concluded that the consistent mass transfer matrix is much superior in accuracy to other transfer matrices in the literature.

4. Parameter identification by transfer matrix method

The proposed TM algorithm is used for identifying the unknown stiffnesses of the structure assuming the masses are known, with negligible damping. The structure is excited at a node with a known harmonic force, and the output responses (acceleration responses) are measured at selected nodes and converted into displacement responses. The initial state vector must be known at one location, preferably near the zone where the stiffness has to be identified. Various strategies of estimating the initial state vector is discussed in the numerical examples given in later sections in this paper. Starting from the known state vector it is possible to predict the displacements at any location in the structure using successive multiplication of the TM's, as discussed in section 2.3. The mean square deviation

between the predicted and measured displacements at a few locations in the structure can be minimized by Particle Swarm Optimization algorithm (PSO) [16]; with the unknown elemental stiffness in the TM as the optimization variables. The TM method of identification can be applied using complete or incomplete set of measurements. "Complete measurement" implies measurement of translational responses at all nodes of the structure (as opposed to a few points in "incomplete measurement"). It is obvious that the numerical accuracy of identification is better with the complete measurement, but due to requirement of large number of sensors it may not be always practical. It is found from numerical examples in the later section that the TM method is capable of satisfactorily identifying parameters from incomplete measurements. The numerical accuracy of identified parameters is reduced, however it is within acceptable bounds; there is also the obvious advantage of speed in this method since identification is carried out in a small locality.

4.1. Simultaneous structural dentification

The entire set of unknown parameters in the structure (or locality near the starting vector) is estimated simultaneously. The mean squared error function between the measured and predicted responses for simultaneous SI is given by

$$\varepsilon = \frac{\sum_{i=1}^{M}\sum_{j=1}^{L}\left|u_m(i,j)-u_e(i,j)\right|^2}{ML} \qquad (33)$$

where $u_m(i,j)$ and $u_e(i,j)$ are measured and estimated displacement responses respectively at i^{th} measurement location and j^{th} time step. M is the number of measurement locations and L is the number of time steps. The mean squared error function is minimized by optimization algorithm. Since all the unknown elemental stiffnesses in the zone of interest are identified simultaneously, more computational effort is required and there is a possibility of increased difficulty in convergence to optimal solution. This method may be suitable for small structures with a set of fewer unknowns. This strategy can be implemented using complete and incomplete measurements.

4.2. Successive structural identification

Here the stiffness of only one (or a few elements) are identified at a time. These elements lie between the initial state vector at one node and the nearest predicted state vector at another node. The optimization algorithm minimizes the error function at only one measurement location at a time. The error function is obtained from Eq.33 by substituting $M=1$and is shown in Eq.34

$$\varepsilon = \frac{\sum_{j=1}^{L}\left|u_m(j)-u_e(j)\right|^2}{L} \qquad (34)$$

Then the cycle is repeated for all the pairs of adjacent measured responses and identify all unknown parameters successively. Since the number of unknown parameters to be identified is one or few for one identification cycle, the convergence is very fast, the overall computational time is very small when compared with simultaneous strategy. This strategy is promising in the identification of local parameters in a structural member. There is of course the question of error propagation in successive identification, however this appears to be balanced out by the superior accuracy per parameter because of smaller size of the problem.

5. Particle swarm optimization (PSO) algorithm

Particle swarm optimization (PSO) is a population based stochastic optimization

technique developed by Eberhart and Kennedy [13]. It is based on the social behavior reflected in flock of birds, bees, and fish that adjust their physical movements to avoid predators, and to seek the best food sources. It is a population based algorithm, in which each particle (unknown stiffnesses or flexural rigidities) is initially positioned randomly over the search space and the number of particles is known as swarm size. The fitness values are calculated using the error function for each particle in the swarm and the particles are ranked according to their fitness values. Particle wise best is known as particle best ($P_{best,k}^{i}$) is selected and is updated at each iteration at each particle. $P_{best,k}^{i}$ means till k^{th} iteration the best in i^{th} particle. After the update of all particle best at every iteration, best of the swarm is called global best particle till k^{th} iteration ($P_{gbest,k}$) is selected and is updated. Each particle is attracted toward the best solution found by the particle's neighborhood and the best solution found by the particle. The position of each particle is adjusted by a stochastic velocity vector which is updated based on the particle best, as well as the best of the swarm is called as Global best as shown in Eq.35 and Eq.36.If x_k^i and v_k^i are the position and velocity of ith particle at k^{th} iteration, then the position and velocity of the same particle at the next iteration can be updated as follows

$$x_{k+1}^{i} = x_k^i + v_{k+1}^{i} \tag{35}$$

$$v_{k+1}^{i} = wv_k^i + c_1 r_1 (P_{best,k}^{i} - x_k^i) + c_2 r_2 (P_{gbest,k}) - x_k^i) \tag{36}$$

where w is linearly varying inertia weight which varies from 0.9 to 0.4 as shown in Eq.37, c_1 is cognitive parameter, c_2 is social parameter both are equal to 2, $r_1$and r_2 are random number in the range of [0; 1][16].

$$w = 0.9 - \frac{0.5(k-1)}{N} \tag{37}$$

Where k is the current iteration and N is the total number of iterations. The updated positions of the particles form the new swarm for the next iteration and the procedure is repeated until the convergence or total number of iterations is completed. PSO records the past history in each particle (P_{best}) as well as swarm (P_{gbest}) in each iteration. Linearly varying inertia term escapes the algorithm from the convergence on local minima and directs toward global minima. The parameters of a Lorenz chaotic system were estimated using PSO [15]. It was found that PSO converges to the exact value with a high population size and was more computationally efficient than GA. Likewise a 10-dof structural dynamic model was identified using frequency response functions by GA and PSO, the PSO was found to be superior to the former in accuracy [14]. Hence the PSO is the good choice as minimizing tool for this SI problem.

5.1. Application of PSO to the current problem

PSO is a heuristic method and superior to classical optimization methods because of its ability to find the global optima. Hence, in this paper PSO is used as the optimizing algorithm. The sequence of operations involved in this problem is illustrated in Figure 5 (a). The objective function here is to minimize the difference between experimentally measured responses and the predicted responses using TM applied to a finite element model. The optimization variables are the unknown stiffness parameters. Each stiffness variable is given a search range of ±50% of its nominal value. Typically 50 particles with 100 iterations are used by PSO to solve the unknown stiffnesses. The detailed flowchart which illustrates the PSO based TM algorithm is shown in Figure 5 (b).

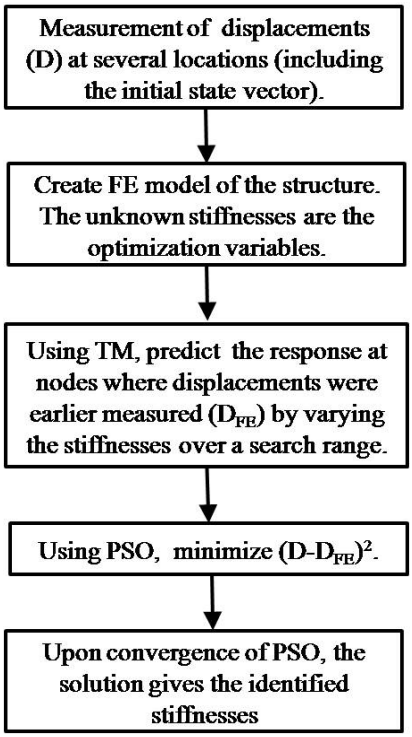

Figure 5. (a). Sequence of operations

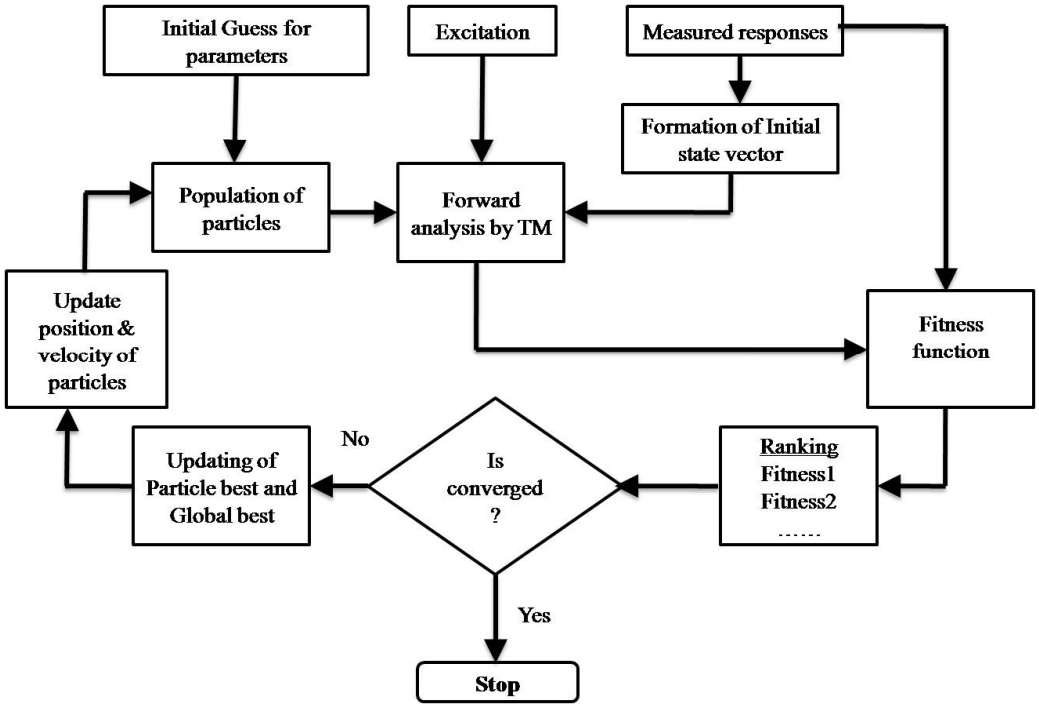

Figure 5. (b). Block diagram for PSO based TM method

6. Numerical examples and results

The TM method is applied on four structures with known forcing and boundary conditions; the last example involves the identification of one member of a nine member framed structure where the strategy of finding the initial state vector is based on strain gauge measurements rather than known boundary conditions. All four are numerically simulated experiments. The structure is excited by a harmonic force at a node and the acceleration responses are measured at selected nodes and converted to displacement responses by numerical integration. In all examples, measured responses are numerically simulated using Newmark's constant acceleration method. The unknown stiffness parameters are searched by PSO algorithm within the search range of ±50% of the nominal stiffness values provided by the user. The displacement responses at all measured nodes are predicted using TM from the initial state vector. The measured and predicted responses are compared and the mean squared error is calculated using Eq.33 or Eq.34 and is the objective function which must be minimized with the unknown elemental stiffnesses in the TM as the optimization variables in PSO. In order to simulate the effect of noise in experiments and also modeling errors, Gaussian random noise with 5% standard deviation and zero mean is added to the measured signals, as is usual in the literature in this area.

6.1. Example-1: 10 DOF lumped mass system

A 10-DOF lumped mass system is first considered which was used by Koh *et al.*[20] with the following parameters as shown in Figure 6. Masses at nodes are m_1 = 600 kg; $m_2 = m_3 = m_4 = m_5$ =400 kg; $m_6 = m_7 = m_8 = m_9 = m_{10}$ = 300 kg. Stiffness of springs are k_1 = 700 kN/m; $k_2 = k_3$ = 650 kN/m; $k_4 = k_5$ = 600 kN/m; $k_6 = k_7 = k_8$ = 400 kN/m; and $k_9 = k_{10}$ = 300 kN/m. The first natural frequency is 1Hz (ω_1= 6.28r/s). Rayleigh damping is adopted with the modal damping ratio of 1%. The system is excited at the tenth mass level by a sinusoidal input force of $F_{10}(t)=10\sin(5.8t)$N. Numerically simulated acceleration responses are obtained for 3*s* at a time step of 0.001*s* using Newmark's constant acceleration method and are converted into displacement responses. The node *10* is chosen for forming initial state vector which is given by $\{X_{10}\} = \{x_{10}(t), F_{10}(t)\}^T$. where $x_{10}(t)$ is the displacement response and $F_{10}(t)$ is the external force, both can be measured using accelerometer and force transducer respectively. Both simultaneous and successive strategies of the TM algorithm are applied on this simple structure with complete and incomplete measurements of responses at selected measurement locations (nodes).

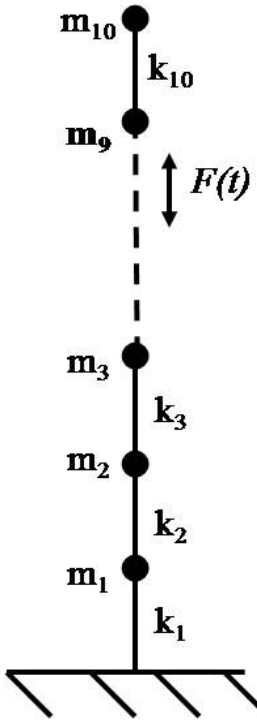

Figure 6. Ten DOF lumped mass system

6.1.1. Simultaneous identification

Responses are measured at all 10 DOF (complete measurement set). The10 unknown stiffnesses are solved simultaneously by the PSO algorithm with a swarm size of 50. Displacement responses at all 10 DOF are predicted from the initial state vector $\{X_{10}\}$ using the transfer matrices according to the Eq.28. The mean squared error between measured and predicted responses at all DOF and each time step is calculated using Eq.33.and is minimized. Since all stiffnesses are identified simultaneously convergence has taken place in 150 iterations and total computational time taken is 17.93s.

It is obvious that the complete measurement of responses at all DOF identifies parameters with very good numerical accuracy, but it is impractical due to large number of sensors. Hence the algorithm should have the capability to identify parameters with incomplete measurement of responses. The simultaneous SI strategy is also applied on the lumped mass system with responses measured at nodes 1, 3, 5, 7, 9 and 10 only. The mean squared error is minimized by PSO only at the above nodes. Since simultaneous identification has 10 unknown parameters to solve, it was necessary to have at least 6 displacement responses for good convergence of solution. About 100 iterations were required for convergence, which took a computational time of 12*s* (less than that of the complete measurement case). The errors are significantly higher, but fewer sensors are needed and computational effort is less. The percentage of error in identified values of stiffness with zero and 5% noise level, from complete and incomplete measurements are shown in Table 2.

Table 2. Percentage of error in identified values of stiffnesses of 10 DOF lumped mass system by simultaneous SI

Element	% of error			
	Complete measurement		Incomplete measurement	
	Without Noise	With 5% Noise	Without Noise	With 5% Noise
1	-0.08	-0.03	-0.92	-0.11
2	-0.02	0.21	0.71	-3.59
3	-0.05	-0.63	-2.68	4.13
4	-0.03	0.64	7.10	-4.52
5	-0.12	0.56	-8.81	4.01
6	0.04	-0.47	6.76	-7.19
7	-0.07	-0.33	-9.27	8.08
8	-0.29	-0.45	-6.31	-9.47
9	-0.97	-0.19	6.11	11.68
10	3.87	-3.29	0.19	-5.25
Mean absolute error	0.55	0.68	4.89	5.80

6.1.2. Successive identification

This strategy is tested with both complete and incomplete response measurements. First with complete set of measurements, algorithm starts from where the initial state vector $\{X_{10}\}$ is formed. The displacement response at the node 9 is first predicted

using Eq.38 and stiffness k_{10} evaluated.

$$\{X_{9i}\} = [T_{10,9}]\{X_{10}\} \quad (38)$$

PSO was used with a swarm size of 50, 30 iterations for each step of identification. In next cycle $\{X_9\}$ becomes known state vector which is used for identification of stiffness k_9. Thus the identification cycle is repeated successively measured responses until all the parameters are identified. For all ten identification cycle 300 iterations are required but takes the computational time is only 3.95s since only one element is solved at a time. This algorithm is suitable for large structures also.

Next, the successive SI is also tested with incomplete set of measurements of responses measured at the nodes 3, 6 and 10 only. From the initial state vector $\{X_{10}\}$, the state vector at the next nearest measured location (*i.e.* node *6*) $\{X_6\}$ is predicted by taking stiffnesses k_7, k_8, k_9 and k_{10} as the unknown parameters and using global transfer matrix for the sub-structure (6-10) of lumped mass system using Eq.29. The mean squared error between measured and predicted responses at the node 6 is minimized by PSO with parameters set in the complete measurement case. This cycle is repeated for the sub-structures (3-6) and (0-3) to identify all the stiffnesses. The total number of iterations would be 90 but the time taken is only 1.58*s* due to only three measurements/cycles. The percentage of error in identified values of stiffness from complete and incomplete measurements is shown in Table 3. The successive identification method with incomplete measurement (which requires the smallest number of sensors and computationally fast) has an error of about 3.4% compared to 4.89% for simultaneous identification. It is clear that the errors can be reduced to 0.3% when using complete set of measurements but it may be impractical with a large number of sensors. Thus the er rors produced by successive identification with incomplete measurements are within a reasonable range, especially when compared to other methods of SI (discussed in the next section).

The following numerical examples use only successive identification strategy.

Table 3. Percentage of error in identified values of stiffnesses of 10 DOF lumped mass system by successive SI

Element	% of error			
	Complete measurement		Incomplete measurement	
	Without Noise	With 5% Noise	Without Noise	With 5% Noise
1	-0.29	0.69	0.80	1.76
2	-0.16	0.13	1.39	6.43
3	-0.28	-0.15	2.34	-5.13
4	0.46	0.83	1.16	-0.55
5	0.13	0.41	7.62	-0.96
6	-0.73	-0.31	-3.35	1.24
7	-0.14	-0.44	0.92	-7.42
8	-0.06	-0.20	-7.73	16.88
9	-0.45	-1.46	5.84	2.95
10	-0.44	0.93	2.76	-7.95
Mean absolute error	0.31	0.56	3.39	5.13

6.1.3. Comparison of results with other time domain methods

Koh *et al.*[20] identified stiffnesses for this problem by using the time domain CSI method as explained in Section.1 from three acceleration responses measured at 2nd, 5th and 10th nodes. GA was used for searching the parameters with population size of 50 and total number of generations was 10,000; stiffnesses were identified with a mean error of 12.5% without noise. It took a total computational time of 220min. Even taking into account the computer hardware, the error is too large compared to the TM method. The TM algorithm with successive identification strategy with known input force identifies stiffnesses from acceleration measurements at 3rd, 6th and 10th nodes only with an error of 5.13% with 5% I/O noise level. It takes 30 trials for each measurement (total 90 trials) and a computational time of 1.58*s*. It shows that this algorithm gives results with improved accuracy at less computational effort from noisy measurement. OKID/ERA [12], another time domain algorithm proposed by Angelis *et al.* which requires complete measurements was applied to this example with the same forcing conditions and time step. The modal damping assumed is 1% of critical damping for first two modes. In noise free condition with complete measurement the stiffnesses were identified with 2.14% mean error which required a time of 97.56*s*. In comparison the TM algorithm with successive strategy produced results with accuracy of 0.31% (Table 3) from complete measurements without noise and the time was 3.95*s*. Hence there appears to be a strong case for the superiority of the TM method.

6.2. Example-2: fixed-fixed beam

A steel beam of Young's modulus 200GPa, length 350mm with uniform cross section, width 24.6mm and thickness 5.7mm, fixed at both the ends, the flexural rigidity (*EI*) of each element is 75.93 N.m^2 with first natural frequency of 243.93Hz (ω_1=1532.6r/s) is discretized into eight elements as shown in Figure 7. The unknown elemental flexural rigidities *EI* (where *E* is the modulus of elasticity and *I* the moment of inertia of the section) have to be identified. It may be noted that although a uniform cross-section beam is assumed, the algorithm makes no assumption of uniform flexural rigidity during identification. The beam is excited by a sinusoidal force of *1.5sin (1250t)*N at its midpoint node, the output acceleration responses are simulated numerically at many locations with a time step of 0.001*s* for 3*s* using Newmark's constant acceleration method. The damping effect is taken into account by adopting Rayleigh damping with the modal damping ratio of 1%.The translational and rotational responses at both fixed ends are zero due to clamped boundary condition, the support reactions of the fixed support is found by principle of superposition technique, hence, all the elements of state vector at any fixed end is known. The initial state vector $\{X_9\} = \{0, 0, M_9(t), V_9(t)\}^T$ is formed at the fixed end (node 9)where $M_9(t)$is the bending moment and $V_9(t)$is the shear force at the right fixed end, calculated using statically determinate force/moment equilibrium conditions. The parameters are identified by successive identification strategy of TM algorithm using single point lumped mass TM and consistent mass TM from both complete and incomplete measurements. Only translational acceleration responses are measured at all nodes for complete measurement. The TM algorithm starts from right end (node 9) and predicts the displacement responses at the node 8 and solves for the *EI* value in-between. The mean squared error is calculated between measured and predicted responses at the node 8 and is minimized by PSO with

swarm size 50and linearly varying inertia weight (0.9-0.4) is used for 50 iterations at each parameter identification cycle. The identification cycle is repeated for other elements. The total computational time is 5.48*s* for complete measurement. The percentage error in identified *EI* values by both single point lumped mass TM and consistent mass TM from complete measurements are tabulated in Table 4. Then the parameters are identified with translational acceleration responses measured at nodes 2, 5 and 7 only. The parameters are identified successively by dividing the beam into four sub-structures such as (7-9), (5-7), (2-5) and (1-2) starting from node 9. Now the total time requirement is reduced to 3.12*s* at the same time the accuracy of the identified results has not reduced significantly. The percentage of error in identified *EI* values by both single point lumped mass TM and consistent mass TM from incomplete measurements are tabulated in the Table 5. The percentage of error in identification using lumped mass TM is 2.36% with complete measurement and 8.34% with incomplete measurement. The same is 2% with complete measurement and 3.13% with incomplete measurement when CMTM is used. In both the cases CMTM produced more accurate results than single point lumped mass TM.

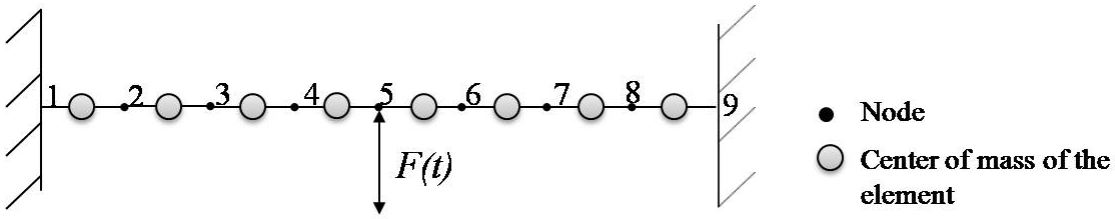

Figure 7. Beam with fixed fixed end

Table 4. Percentage of error in identified values of EI of fixed beam from complete measurement

Element	% of error			
	Lumped mass TM		Consistent mass TM	
	Without Noise	With 5% Noise	Without Noise	With 5% Noise
1	0.09	3.84	0.02	3.01
2	-3.44	1.40	-3.29	-7.44
3	1.33	-1.38	1.50	2.86
4	0.14	0.29	0.12	-0.09
5	0.19	2.43	0.21	-0.39
6	-0.09	-6.19	-0.09	1.73
7	0.26	-2.81	0.26	-0.31
8	0.19	0.57	0.19	0.16
Mean absolute error	0.72	2.36	0.71	2.00

Table 5. Percentage of error in identified values of EI of fixed beam from incomplete measurements at nodes 2, 5 and 7 only

Element	% of error			
	Lumped mass TM		Consistent mass TM	
	Without Noise	With 5% Noise	Without Noise	With 5% Noise
1	9.36	17.45	1.13	-8.38
2	-1.93	19.95	-6.72	0.62
3	-1.82	-3.01	-1.19	-7.49
4	4.43	-1.49	-3.89	-2.98
5	-2.83	4.14	5.44	-2.57
6	-3.87	6.26	-2.59	1.48
7	-7.29	13.04	-0.27	1.47
8	1.36	-1.40	0.27	0.02
Mean absolute error	4.11	8.34	2.69	3.13

6.3. Example-3: cantilever

A cantilever which is used in section.3 is considered for parameter identification as shown in Figure 8. The natural frequencies of the cantilever are shown in Table 1. The beam is excited by a sinusoidal force of *1.5sin(62.83t)* N at its free end node. The damping effect is taken into account by adopting Rayleigh damping with the modal damping ratio of 1%. The translational accelerations are measured at all nodes; at the free end both translational and rotational response is measured to define the initial state vector. The bending moment at the free end is zero and the shear force there is equal to input excitation force hence, all the elements of state vector at free end are known, $\{X_8\}=\{y_8(t);\ \theta_8(t);0;\ F(t)\}^T$. Note that $y_8(t)$ and $\theta_8(t)$ have to be measured from accelerometers at the free end. From the initial state vector the unknown parameters are identified using single point lumped mass TM and consistent mass TM successively as explained in the above example with PSO parameters of 50 iterations in each identification cycle; hence the total number of iterations is 350. The identification algorithm is repeated with translational responses measured at nodes 3, 5, 7 and 8. The cantilever is divided into four substructures from nodes (1-3), (3-5), (5-7) and (7-8) and parameters are identified as explained in the Example.2. The total computational time is 4.8*s* with complete measurements and the computational time is 3.12s with incomplete measurements. The percentage of mean absolute error of identified values from complete and incomplete measurements is tabulated in Table 6. The error in case of incomplete measurement is more (3.07%) when compared to that of complete measurements (0.83%) using CMTM, but it is not significantly large. When the lumped mass TM is used for identification, the error is 2.66% for complete measurement case and 5.48% for incomplete measurement case. In this example also it has been proved that the consistent mass TM is superior to single point lumped mass TM.

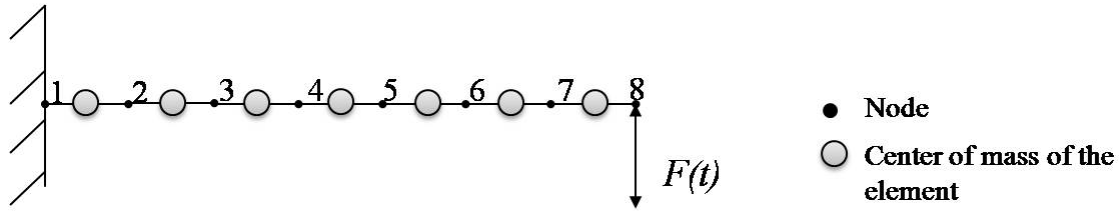

Figure 8. Cantilever with seven elements

Table 6. Percentage of mean absolute error in identified values of EI of cantilever

Measurement Type	% of error			
	Lumped mass TM		Consistent mass TM	
	Without Noise	With 5% Noise	Without Noise	With 5% Noise
Complete	0.21	2.66	0.06	0.83
Incomplete	2.35	5.48	1.78	3.07

6.3.1. Variation of error with respect to variation of frequency ratio

The dependence of percentage of mean absolute error of identified flexural rigidities of the cantilever on the ratio of frequency of excitation to the first natural frequency (ω/ω_1) is shown in Figure 9. It is seen that the error slowly increases with high frequency ratio. This could be probably due to the error in neglecting the angular displacements at higher frequencies. It may be recalled that only the translational displacements are predicted and matched against measured observations.

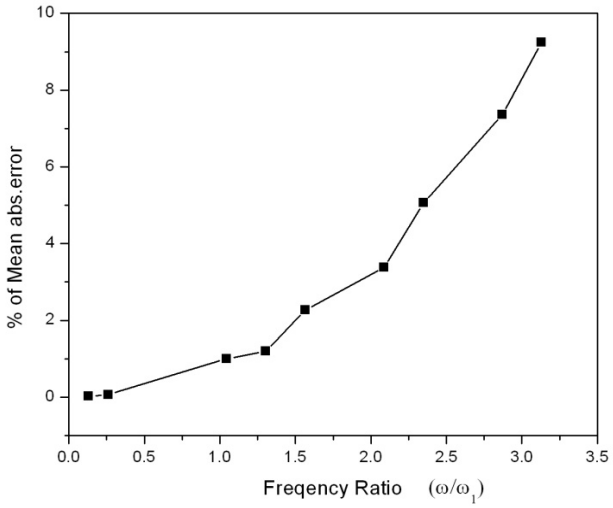

Figure 9. Variation of error with respect to ratio of exciting and first natural frequencies

6.4. Example: 4 – identification of member stiffnesses of a frame structure

A frame steel structure made of nine members is rigidly fixed at two supports as shown in Figure 10 (a) and it taken from Prashanth and Shankar [30]. Each member has a cross section of *12* × *6* mm and a flexural rigidity (*EI*) of 43.2 N.m^2. The first natural frequency is 11.9 Hz. It is proposed to identify the stiffnesses of the top horizontal member 4, which has a length of 1m. The zone of identification is indicated by a box in Figure 10 (a) covering 0.875m. The structure is excited by a sinusoidal input force of *10sin(62.83t)* N at the midpoint of the member 6. The damping effect is taken into account by adopting Rayleigh damping with the modal damping ratio of 1%. Member 4 of the structure is separated is divided into seven elements as shown in Figure 10 (b). The initial state vector need be formed at any arbitrary node in member 4 which requires measurement of translational and angular responses, as well as shear force and bending moment responses at that node. The first two responses can be measured directly by accelerometers and last two responses have to be measured by strain gauges *i.e,* by measuring strain responses [31] as explained below.

6.4.1. Measurement of shear force and bending moment responses

For a rectangular section beam, the bending strain response is given by

$$\varepsilon_B(t) = \frac{M(t)y}{EI} \tag{39}$$

Where, $M(t)$ is the bending moment, EI is the flexural rigidity and $y = h/2$, h is the depth of the beam section.

$$M(t) = \frac{2EI\varepsilon_B(t)}{h} \tag{40}$$

The shear force in the section is given by

$$V(t) = \frac{8EI\varepsilon_S(t)}{h^2(1+\nu)} \tag{41}$$

Where, ε_S is the shear strain and ν is Poisson's ratio. Bending moment and shear force could be measured through strain gauges. From Eq.40 and 41, it is understood that calculating the bending moment and shear force responses at the starting node require knowledge of the flexural rigidity (*EI*) at that portion. There are two options here (a) assume that the *EI* at the starting node is known in which case (b) estimate the *EI* value in the vicinity of the starting node using a simple shear strain test as is presented here. In this case strain gauges are fixed close to each other at *A* and *B* (Figure 11) in a small zone; point B coincides with node-8 where the initial state vector is to be obtained. For shear measurement, 4 strain gauges with 90^0 orientation between them [31] could be used and it is capable of measuring minute strains. At a point *C*, in between *A* and *B*, a static load *W*=10 *kN* is applied and the corresponding shear strains at the sections *A* and *B* are measured (in the numerically simulated example, these shear strains are generated from a known finite element model of the frame). It is assumed that the flexural rigidity is uniform between the points *A* and *B* also the self-weight of the portion *AB* is negligible compared to *W*. The change in shear force at sections *A* and *B* is equal to the applied load *W* at *C*. From Eq.41,

$$V_A - V_B = \frac{8EI(\varepsilon_{SA} - \varepsilon_{SB})}{h^2(1+\nu)} \tag{42}$$

$$EI = \frac{Wh^2(1+\nu)}{8(\varepsilon_{SA} - \varepsilon_{SB})} \tag{43}$$

From Eq.43 the flexural rigidity in the vicinity of the starting node-8 can be calculated; and using this value in Eq.40 and 41 shear force and bending moment can be readily obtained for any strain values at node-8. After this initial estimation of *EI*, the strain gauge A is not necessary anymore;

only strain gauge B at node-8 is required to calculate the dynamic strains from which bending moment and shear forces can be calculated and used in the initial state vector at node-8.

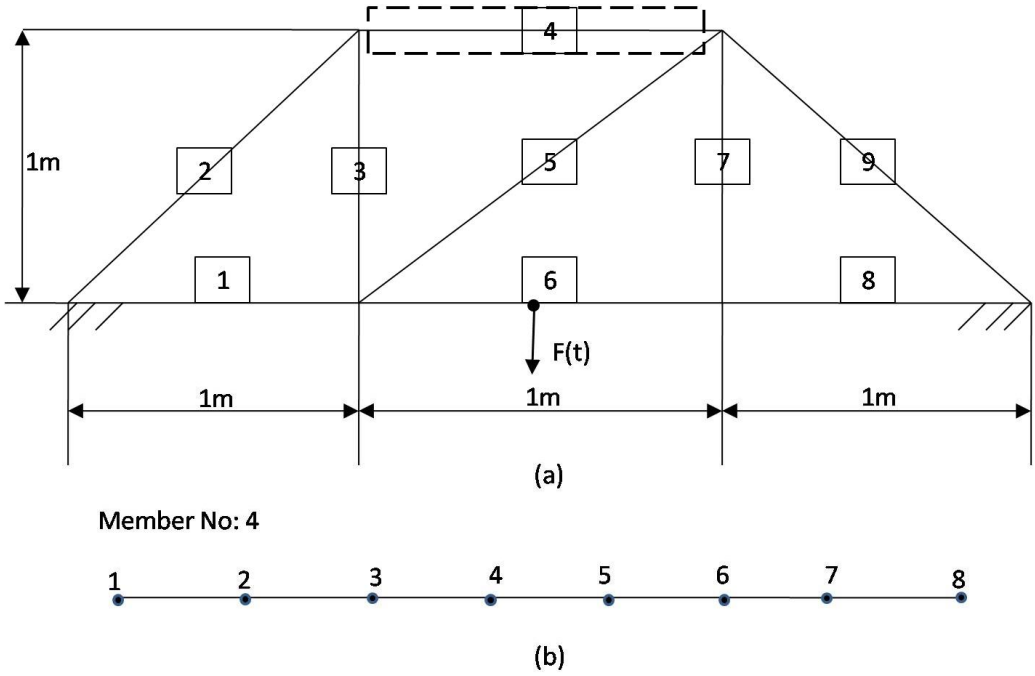

Figure 10. (a). Global structure (b). Member of the global structure

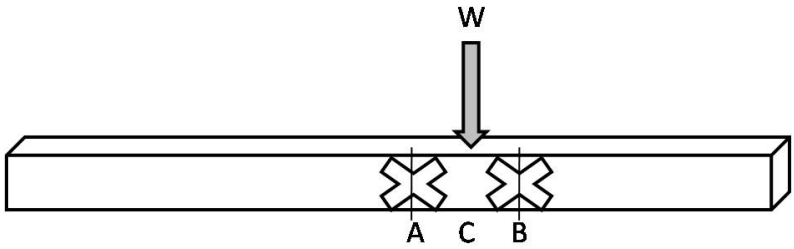

Figure 11. Strain gauge arrangement for identification of initial EI

6.4.2. Successive identification

The eighth node on the member 4 inFigure 10 (b) is chosen for the initial state vector. The translational and angular displacements, bending moment and shear force responses are measured at that node as explained previously and initial state vector $\{X_8\} = \{y_8(t);\ \theta_8(t);\ M_8(t);V_8(t)\}^T$ is formed . The translational acceleration at all other nodes in Figure 10 (b) are also measured. Using PSO with a swarm size of 50, successive *EI* values are obtained sequentially as mentioned in the previous examples. Number of iterations per cycle was 50; the total time of identification for seven *EI* values with complete measurement was 5.55*s*.

The same example is identified with incomplete measurements also. Translational displacement measurements at nodes 1, 3, 5 and 8 are used here. The

structure is divided into three portions between nodes (1-3), (3-5) and (5-8). The SI algorithm starts from the initial state vector at the node 8 and identifies parameters of each portion successively. PSO used a swarm size of 50 and 100 iterations in each cycle. The total computational time is 7.56*s*. The percentage of mean absolute error in identified parameters is tabulated in Table 7 for both complete and incomplete measurements. It is seen that the error incurred when using non-noisy incomplete measurement (3.13%) is higher than with the complete measurement (0.14%); but still in the acceptable range compared to other SI methods. Incomplete measurement requires only 5 sensors and produced results with acceptable error. This shows that the TM algorithm is suitable for the identification of local parameters of complex structure. It may be noted that Prashanth and Shankar [30] had identified this problem with a 2 stage neural network trained with time domain acceleration signals at two nodes; the mean error of identification incurred in that method was about 2% for non-noisy signal but the computational effort of training the network and the complexity of 2 stage network has to be contrasted with the simplicity of the TM method.

Although the TM for only lumped mass systems and beams are presented here, it could be derived for truss element, plate element etc., Hence the method can be readily extended to many type of engineering structures. The advantage of the TM method is that we can locally identify the damage without analyzing the entire structure. This method can also be used to detect cracks by deriving the TM for cracked structural elements for which finite element formulation is available. These are the some of the potential areas of future application of this method.

Table 7. Percentage of mean absolute error in identified values of EI of inner member of structure

% of error			
Complete measurement		Incomplete measurement[a]	
Without Noise	With 5% Noise	Without Noise	With 5% Noise
0.14	2.20	3.13	5.09

[a] responses measured at nodes 1, 3, 5 and 8 only

7. Conclusion

A novel structural identification technique using transfer matrix (TM) and state vector has been presented. An accurate TM based on consistent mass representation (CMTM) has been developed. In the identification process the initial state vector has to be provided, and displacement at any node in the structure is predicted using TM, and the deviations from the measure values are minimized with the unknown stiffnesses as the optimization variables. Two different strategies such as simultaneous and successive structural identification are investigated with complete and incomplete measurements of responses; the accuracy is studied with four numerically simulated experiments. The successive identification scheme is shown to give good accuracy coupled with small computational effort, compared with other time domain methods in the literature. In some examples the initial state vector is readily obtained from simple boundary conditions. But in a nine member frame structure, the initial state vector is derived from strain gauge measurements. It is concluded that the TM algorithm with successive identification using CMTM is a promising method for structural

identification. It has the ability of identification of local parameters in a portion of a big structure, without the requirement of knowing the global properties.

Acknowledgment

The authors gratefully acknowledge the research grant provided by Council for Sci

entific and Industrial Research (CSIR), New Delhi.

References

[1] Aditya, G. and Chakraborty, S. 2008. Sensitivity Based Health Monitoring of Structures with Static Response. *Scientia Iranica* 15, 3: 267-274.

[2] Hjelmstad, K. D. and Shin, S. 1997. Damage Detection and Assessment of Structures from Static response. *Journal of Engineering Mechanics*, 123, 6: 568-576.

[3] Maia, N. M. M. and Silva, J. M. M. 2001. Modal Analysis Identification Techniques. *Philosophical Transactions of the Royal Society*, 359: 29-40.

[4] Ma, G. and Eric, M. L. 2005. Structural damage identification using system dynamic properties. *Computers and Structures*, 83: 2185–2196.

[5] Jinhee, L. Identification of multiple cracks in a beam using vibration amplitudes. Journal of Sound and Vibration, 326: 205-212.

[6] Ghanem, R. and Shinozuka, M. 1995. Structural system identification I: Theory. *Journal of Engineering Mechanics*, 121, 2: 255-264.

[7] Petsounis, K. A. and Fassois, S. D. 2001. Parameteric Time-Domain Methods for the Identification of Vibrating Structures-A Critical Comparison and Assessment. *Mechanical System and Signal Processing,* 15, 6: 1031-1060.

[8] Caravani, P., Watson, M. L., and Thomson, W.T. 1977. Recursive Least square Time domain Identification of structural Parameters. *Journal of Applied Mechanics,* 44, 1: 135-140.

[9] Masaru, H. and Etsuro, S. 1984. Structural Identification by Extended Kalman Filter. *Journal of Engineering Mechanics*, ASCE110, 12: 1757-1770.

[10] Shinozuka, M., Yun, C. B., and Imai, H.1982. Identification of Linear structural dynamic system. *Journal of Engineering Mechanics*, ASCE108, 6: 1371-1390.

[11] Lus, H., Betti, R., and Longman, R. W. 1999. Identification of Linear Structural Systems Using Earth quake-induced Vibration Data. *Earthquake Engineering and Structural Dynamics*, 28: 1449-1467.

[12] Angelis, M. De., Lus,H., Betti.R., and Longman, R. W. 2002. Extracting Physical Parameters of Mechanical Models from Identified State-Space Representations. *Journal of Applied Mechanics*, 69: 617-625.

[13] Kennedy,J. and Eberhart R. 1995. Particle swarm optimization. Presented in IEEE international conference on neural networks, (IV) Piscataway, NJ, : 1942-1948.

[14] Mouser, C. R. and Dunn, S. A., 2005. Comparing Genetic Algorithm and Particle Swarm Optimization for Inverse Problem. *ANZIAM Journal*, 46: 89-101.

[15] Qie, H., Ling, W., and Bo. L., 2007. Parameter Estimation for Chaotic Systems by Particle Swarm Optimization. *Chaos, Solitons and Fractals*, 34: 654–661.

[16] Perez, R. E. and Behdinan, K. 2007. Particle Swarm Approach for Structural Design Optimization. *Computers and*

Structures, 85: 1579-1588.

[17] Koh,C.G., Chen,Y.F. and Liaw, C. Y. 2003. A hybrid Computational Strategy for identification of Structural parameters. *Computers and Structures*, 81: 107-117.

[18] Begambre, O. and Laier, J.E. 2009. A hybrid Particle Swarm Optimization-Simplex Algorithm (PSOS) for Structural damage Identification. *Advances in Engineering Software*, 40: 883-891.

[19] Hesheng, T., Songtao., X., and Cunxin, F. 2008. Differential evolution Strategy for Structural System Identification. *Computers and Structures*, 86: 2004-2012.

[20] Koh,C.G., Hong, B., and Liaw, C. Y. 2003. Substructural and Progressive structural Identification Methods. *Engineering Structures*, 25: 1551-1563.

[21] Koh, C. G., Hong, B., and Liaw, C. Y. 2000. Parameter Identification of Large Structural Systems in Time Domain. *Journal of Structural Engineering*, 126, 8: 957-963.

[22] Sandesh, S. and Shankar, K.2009. Damage Identification of a Thin Plate in the Time Domain with Substructuring-an Application of inverse Problem. *International Journal of Applied Science and Engineering*, 7: 79-93.

[23] Tee, K. F., Koh, C. G., and Quek, S. T. 2009. Numerical and Experimental Studies of a Substructural Identification Strategy. *Structural Health Monitoring*, 8, 5: 397-414.

[24] Steidel, R. F. 1978. "A*n Introduction to Mechanical Vibrations*". Second Ed., John Wiley and Sons, U.S.A.

[25] Meirovitch, L. 2001. "*Fundamentals of Vibrations*". First Ed., McGraw-Hill Book Company.

[26] Nandakumar, P. and Shankar, K. 2011. Identification of Structural Parameters Using Transfer Matrix and State Vectors in Time Domain. *Presented in the 5th International Conference on Advances in Mechanical Engineering*, Surat, India, June 6th to June 8th , 2011.

[27] Khiem, N.T. and Lien, T.V. 2001. A Simplified method for Natural Frequency Analysis of a Multiple cracked Beam. *Journal of sound and vibration,* 245, 4: 737-751.

[28] Tuma, J. J. and Cheng, F.Y. 1982. "*Theory and Problems of Dynamic structural analysis*". McGraw-Hill Book Company.

[29] Walter, W. and Walter, D. P. 2003. "*Mechanics of Structures Variational and Computational Methods*". 2nded, CRC Press.

[30] Prashanth, P. and Shankar, K. 2008. A Hybrid Neural Network Strategy for the Identification of Structural Damage using Time Domain Responses. *IES Journal Part A: Civil and Structural Engineering*, 1, 4: 17-34

[31] Positioning strain gages to monitor bending, axial, shear and torsional loads. available at: www.omega.com/faq/pressure/pdf/positioning.pdf